Available online at www.sciencedirect.com
SCIENCE DIRECT®
Nuclear Instruments and Methods in Physics Research A 557 (2006) 23–27
NUCLEAR INSTRUMENTS & METHODS IN PHYSICS RESEARCH Section A
www.elsevier.com/locate/nima

Status of the Novosibirsk energy recovery linac

V.P. Bolotin, N.A. Vinokurov*, N.G. Gavrilov, D.A. Kayran, B.A. Knyazev, E.I. Kolobanov, V.V. Kotenkov, V.V. Kubarev, G.N. Kulipanov, A.N. Matveenko, L.E. Medvedev, S.V. Miginsky, L.A. Mironenko, A.D. Oreshkov, V.K. Ovchar, V.M. Popik, T.V. Salikova, S.S. Serednyakov, A.N. Skrinsky, O.A. Shevchenko, M.A. Scheglov, V.G. Tcheskidov

Budker Institute of Nuclear Physics, 11 Lavrentyev Prospect, Novosibirsk 630090, Russia

Available online 15 November 2005

Abstract

The Novosibirsk terahertz free electron laser is based on the energy recovery linac (ERL) with room-temperature radiofrequency system. Some features of the ERL are discussed. The results of emittance measurements and electron optics tests are presented. The second stage of the ERL, which has four orbits, is described briefly.

PACS: 41.60.Cr

Keywords: Recirculating linacs; Free electron lasers

1. Introduction

A new source of terahertz radiation was commissioned recently in Novosibirsk [1]. It is CW FEL based on an accelerator–recuperator or an energy recovery linac (ERL). It differs from the earlier ERL-based FELs [2,3] in the low-frequency non-superconducting radiofrequency (RF) cavities and longer wavelength operation range. Full-scale Novosibirsk free electron laser is to be based on the four-orbit, 40 MeV accelerator–recuperator (see Fig. 1). It is to generate radiation in the range 5 μ–0.2 mm [4,5].

2. Accelerator–recuperator

The first stage of the machine has a full-scale RF system, but has only one orbit. Layout of the accelerator–recuperator is shown in Fig. 2. The 2 MeV electron beam from an injector passes through the accelerating structure, acquiring the 12-MeV energy, and comes to the FEL, installed in the straight section. After interaction with radiation in the FEL, the beam passes once more through the accelerating structure, returning the power, and comes to the beam dump at the injection energy. Main parameters of the accelerator are listed in Table 1.

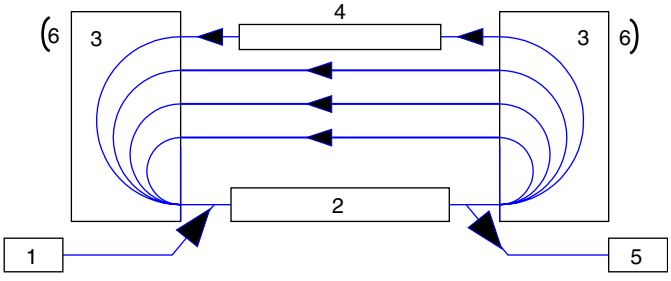

Fig. 1. Scheme of the accelerator–recuperator-based FEL. 1—injector, 2—accelerating RF structure, 3—180° bends, 4—undulator, 5—beam dump, 6—mirrors of the optical resonator.

3. Injector

The electron source is the 300 keV DC gun with gridded cathode. The electron gun consists of

- a cathode-grid unit driven by a controlled pulser,
- an electrostatic accelerating tube placed in a high-pressure vessel with insulating SF_6 gas,

*Corresponding author. Tel.: +7 3832 394003; fax: +7 3833 307163.
E-mail address: vinokurov@inp.nsk.su (N.A. Vinokurov).

0168-9002/$ - see front matter © 2005 Elsevier B.V. All rights reserved.
doi:10.1016/j.nima.2005.10.056

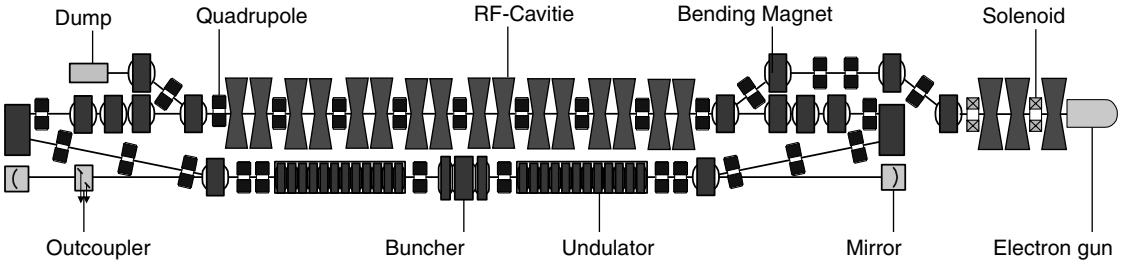

Fig. 2. Scheme of the first stage of the Novosibirsk high-power FEL.

Table 1
Accelerator parameters (first stage)

RF frequency (MHz)	180
Number of RF cavities	16
Amplitude of accelerating voltage at one cavity (MV)	0.7
Injection energy (MeV)	2
Final electron energy (MeV)	12
Maximum bunch repetition rate 9MHz)	11.3
Maximum average current (mA)	20
Beam emittance (mm mrad)	2
Final electron energy spread, FWHM (%)	0.2
Final electron bunch length (ns)	0.1
Final peak electron current (A)	10

- a 300 kV DC power supply, and
- a control electronics inside the high-voltage terminal with the optical link.

The main parameters of the gun are

Electron energy (kinetic)	300 keV
Current:	
Peak	1.25 A
Average	40 mA
Normalized emittance	30π mm mrad
Repetition rate	0…22.5 MHz
Pulse duration	1.6 ns
Operation mode	CW

The gridded cathode of the commercial RF tube is used as the source of short electron bunches. The home-made pulser provides 1.5 ns 100 V pulses at the cathode (the grid is grounded). As such, a pulse (bunch) duration is too long for the RF acceleration; at a frequency of 180 MHz, bunch compression is necessary. The simplest way to do it—the klystron bunching at the same frequency—was chosen. The gun voltage of 300 kV is a trade-off between suppression of the space charge-induced emittance degradation and the possibility to compress the bunch in the drift space (without magnetic buncher). The RF voltage on the bunching cavity is about 100 kV. After the 3 m drift space, two accelerating cavities are installed. They ramp the beam energy to 1.7 MeV.

4. Emittance measurements

The beam quality is one of the important issues for all ERL applications and for better understanding of the energy recovery efficiency. Therefore, the emittance measurements were carried out.

When the first bending magnet is switched off, the electron beam from the injector falls to the water-cooled copper plate (normal incidence). The optical transition radiation is observed at the angles near 60° to the plate normal. The beam emittance is measured at low bunch repetition rate (usually 22 kHz, which is the lowest possible frequency at the installation now, or a small multiple of it).

The beam density distribution is measured at different currents in focusing solenoids or quadrupoles before the OTR screen. For the beam size measurement, we use standard CCD camera (calibrated to give linear response) and a video adapter with a frame grabbing capability. The pictures of the beam are stored in a single ".avi" file. This file is processed further by a MATLAB program with graphical user interface, which allows to set all necessary parameters and to choose the approximation method for the density distribution (standard distributions as Gaussian or waterbag can be chosen or, alternatively, the RMS beam size is calculated).

The beam parameters (horizontal and vertical emittances and Twiss parameters) can be calculated from the dependence of the beam sizes on the optical strength of the nearest electron lens. The square of size is parabolic with respect to the lens strength (if the space charge is negligible). By fitting the measured squared beam sizes by a parabola, one can get the beam Twiss parameters of the lens. Practically, beam size measurement, residual magnetic fields, lens aberrations, and space charge effects are the problems to deal with by the data processing.

An example of the measurement results is shown in Fig. 3. The current in a focusing solenoid before the bend is varying. Bunch charge was reduced to about 0.3 nC and bunching resonator was switched off in this experiment to decrease the space charge effects. Accelerating RF cavities were also switched off (the beam energy was about 280 keV).

In this example, the measured emittances are $\varepsilon_x = 14$ and $\varepsilon_y = 16$ microns, $\beta_x = 7.2$ m, $\alpha_x = 5.1$, $\beta_y = 4.1$ m, $\alpha_y = 3.3$. The Gaussian distribution was chosen to fit the

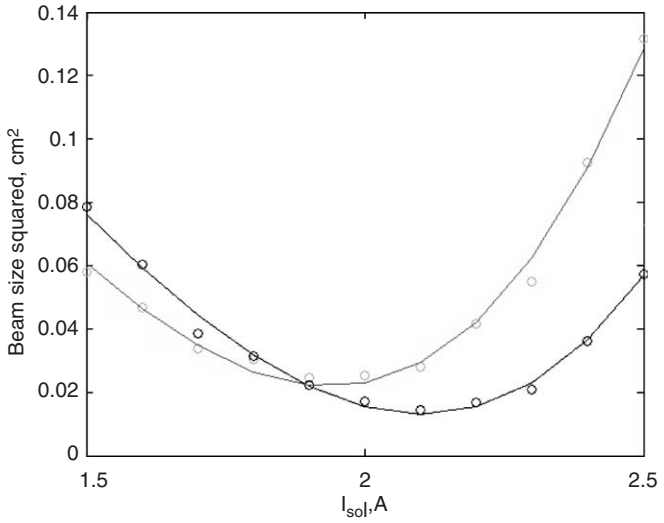

Fig. 3. Squared beam size vs. focusing solenoid current. Circles are measured points for x and y direction, lines are approximations.

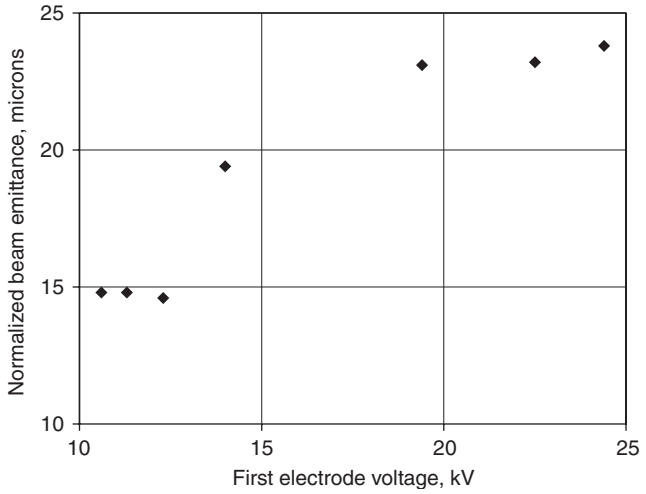

Fig. 4. Normalized beam emittance vs. the first accelerating electrode voltage.

measured beam profile. (If the RMS beam size is calculated, the resulting emittance is somewhat smaller (about 30%), but it is the matter of definition.)

Although the statistical error of the measured beam parameters is small ($<5\%$), systematic errors must be eliminated to give accurate results. Two of the possible sources of error seem to be of most importance for us. First is the camera resolution. It must be taken into account especially for a high-energy (i.e., low emittance) beam in the injector. Although we have only solenoid optics in the injector, the beam vertical and horizontal Twiss parameters and emittances in Fig. 3 are different. We suppose this difference to be due to residual fields in a quadrupole located between the last solenoid and the OTR screen, which was switched off, but not demagnetized, during the experiment.

Emittance measurements were carried out for different voltages on the first accelerating electrode in the gun. The first OTR screen located after the first solenoid was used for the measurements. The voltage was controlled by a passive dividing circuit. The first resistor in the dividing chain was shunted by a controlled kenotron tube. By changing the tube current, one can change the accelerating field on the cathode grid, which influences the beam emittance. All the other parameters of the gun are in our usual operating regime. The bunch charge was about 1.25 nC, and the beam energy 280 keV. The results are shown in Fig. 4.

The measurements of the beam emittance dependence on the bunch charge (i.e., the cathode–grid accelerating gap voltage) was attempted, but no visible effect on the beam emittance was found. At the same time, the beam Twiss parameters changed significantly. For example, at the bunch charge 1.25 nC, $\varepsilon = 23.3\,\mu$, $\beta = 5.9$ m, and $\alpha = -8.0$ m, and at 0.3 nC, $\varepsilon = 23.8\,\mu$, $\beta = 3.0$ m, and $\alpha = -3.7$ m (the measurements were made at the first

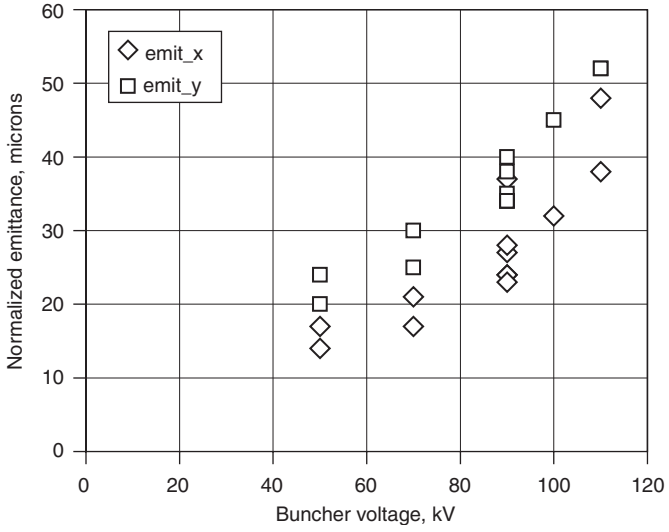

Fig. 5. Normalized beam emittance vs. buncher voltage amplitude. Diamonds are horizontal, squares are vertical emittances. Multiple measurements at the same voltage were made by different beam optics in the channel.

accelerating electrode voltage 24 kV, other parameters are the same as for Fig. 4.) It means that space charge defocuses the beam, but does not change the emittance significantly. The emittance appears at the grid in this case. The simple estimations of the emittance growth at the grid confirm this.

A number of emittance measurements of the 1.7 MeV beam accelerated in the injector were made. During these measurements, we attempted to optimize the beamline optics and RF phases to minimize the emittance growth. Some of the results are shown in Fig. 5. Here, the dependence of the emittance on the bunching RF cavity voltage amplitude is depicted. The accelerating amplitude on each of the two accelerating RF cavities in the injector

was 605 kV. The measurements showed that the emittance is better at lower buncher voltages. However, the bunch length must be shortened to increase the peak current and to decrease the longitudinal emittance degradation during acceleration. So, a buncher amplitude of 80 kV is used in the FEL operating regime.

Up to now, a number of emittance measurements were carried out in the injector to optimize the beam optics. The main results are the following:

1. beam density distribution in a bunch is close to parabolic (waterbag distribution),
2. RF cavities phase and the buncher amplitude tuning can vary the beam normalized emittance from 15 to 50 μ, and
3. the injector beam optics must be controlled to maintain the beam quality.

Experiments to improve the beam quality for FEL operation will be continued.

5. Optics measurements

A series of experiments on beam optics measurements were carried out. They are necessary to obtain the design beam envelopes. The last issue is especially important for the matching of the beam at strong-focusing undulators and at the last stage of the beam deceleration and its transport to the dump. All the following experiments were made at a minimal beam repetition frequency 22 kHz at the usual working bunch charge of about 1.5 nC.

First, the beam dispersion function was measured at the first beam position monitor (BPM) after the first bending magnet in the injector. The measurements were carried out for different strengths of the quadrupole located between the magnet and the BPM. The beam energy was changed by a decrease of the accelerating field amplitude of the last RF cavity of the injector. The time-of-flight factor 0.9 for the cavities was used to find the beam energy variation. The measurements showed good agreement with calculations and allowed deriving the beam energy with the accuracy of about 5%.

Second, combinations of transport matrix elements were measured by the following procedures:

1. a steering coil (corrector) strength was periodically changed, that led to the downstream trajectory change,
2. the trajectory displacement at a BPM was observed, and
3. the strength of a lens between the corrector and the BPM was adjusted to minimize the orbit displacement at the BPM.

The scheme of the experiment is shown in Fig. 6. Here, A and B denote matrixes of the system between the corrector and the lens, and the lens and the BPM, respectively. In the thin lens approximation, the lens strength may be expressed through the matrix elements as $P = b_{22}/b_{12} + a_{11}/a_{12}$.

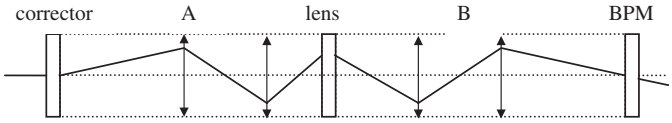

Fig. 6. Transport matrix elements measurement scheme.

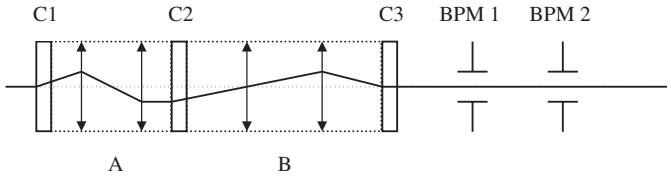

Fig. 7. Corrector triples coefficients measurement scheme. C1, C2, and C3 are the correctors of the triple, A and B are the transport matrixes of the system between correctors. Two BPMs are used to control so that the downstream beam trajectory does not change.

This method is independent of the BPM calibration. However, pickup noises must be reduced as far as possible to improve the accuracy. Since the lens strength is detuned from the normal operation regime, some adjacent optics must be adjusted to keep the beam losses low. This is an additional complication of the scheme.

The measured value of P was compared to a calculated value. The beam energy was the free parameter in the calculations and it can be derived from the measurement results processing. The results achieved in a number of experiments are consistent.

Third, steering coils triples coefficients were measured. The scheme of the experiment is shown in Fig. 7. The beam trajectory is deflected by an angle $\delta x'$, and is returned on the basic trajectory by deflecting angles $\alpha\,\delta x'$ and $\beta\,\delta x'$ with two other correctors. The beam trajectory is controlled by two downstream pickups. The coefficients α and β are given by $\alpha = -b_{11}a_{12}/b_{12} - a_{22}$, $\beta = a_{12}/b_{12}$, where a and b are the matrix elements of the transport matrixes A and B, respectively.

The coefficients were determined experimentally by measuring the beam displacement at the BPMs when each corrector bends the trajectory by $\delta x'$. The 3×2 matrix of displacements is produced this way. Singular Value Decomposition procedure applied to the matrix gives the null-space vector of the matrix which is the normalized $(1, \alpha, \beta)$ vector [6]. The beam position was averaged over 50 measurements to improve the accuracy.

6. Second stage of the ERL

The design and manufacturing of the full-scale four-turn ERL is underway. An artistic view of the machine is shown in Fig. 8. The existing orbit with the terahertz FEL lies in the vertical plane. The new four turns are in the horizontal one. When the round separating magnets are switched on, the beam does not go to the old terahertz FEL, but to the

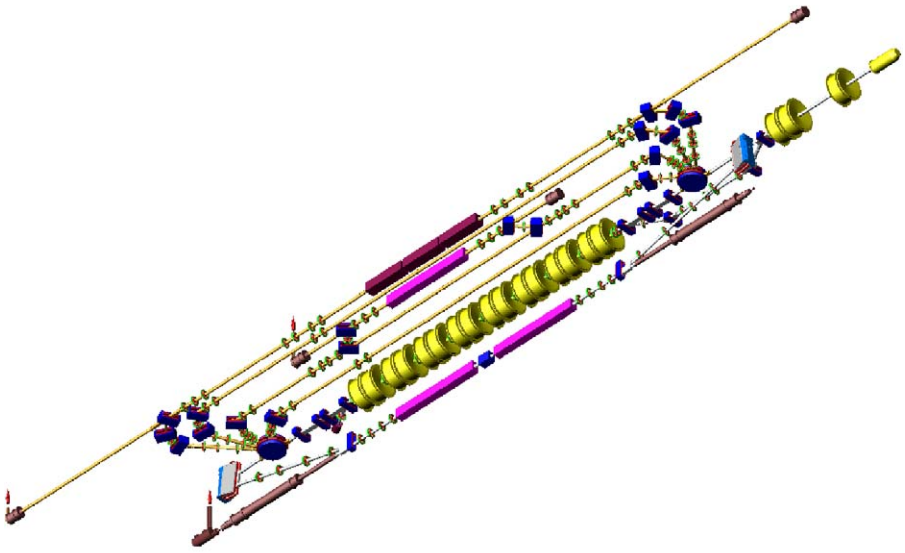

Fig. 8. The second stage of the Novosibirsk high-power FEL (bottom view).

new horizontal turns. One FEL is installed at the fourth orbit (40 MeV energy), and the second one at the bypass of the second orbit (20 MeV energy).

Acknowledgment

This work was supported by the integration grant no. 174 of the Siberian Branch of Russian Academy of Science.

References

[1] E.A. Antokhin, et al., Nucl. Instr. and Meth. A 528 (2004) 15.
[2] G.R. Neil, et al., Phys. Rev. Lett. 84 (2000) 662.
[3] E.J. Minehara, Nucl. Instr. and Meth. A 483 (2002) 8.
[4] N.G. Gavrilov, et al., IEEE J. Quant. Electron. QE-27 (1991) 2626.
[5] V.P. Bolotin, et al., Proceedings of FEL-2000, Durham, USA, 2000, pp. II–37.
[6] F. Zimmerman, in: Beam Measurement, World Scientific. Proceedings of the Joint US-CERN–Japan–Russia School on Particle Accelerators, Switzerland, 1998, pp. 21–107.